This article has been accepted for publication in a future issue of this journal, but has not been fully edited. Content may change prior to final publication. Citation information: DOI 10.1109/TVT.2018.2881318, IEEE Transactions on Vehicular Technology

Gaussian Mixture Model for Millimeter-Wave Cellular Communication Networks

Xiang Liu, Jing Xu, Yiyang Pei, *Member, IEEE*, and Ying-Chang Liang, *Fellow, IEEE*

***Abstract*—As compared to the microwave communication networks, the theoretical analyses of system performances such as the cell coverage and the cell average data rate are more difficult due to the unique propagation path loss model for mmWave cellular communication networks. In this paper, based on the unique transmission states of the distance-dependent piecewise propagation probability functions, the analytical six-state analytical mixture distribution of the propagation loss including the distance-dependent path loss, shadowing and small-scale fading is obtained. For each state, a novel Kullback-Leibler divergence based Gaussian approximation method is proposed to model the distribution of the propagation loss. The distribution of the propagation loss including the large-scale fading and small-scale fading is approximated via a six-state Gaussian mixture model, then the closed-form expression for the signal-to-noise ratio can be easily obtained. The cell coverage is expressed as the weighted sum of the error functions, and the cell average data rate is expressed as the weighted sum of the moments of the propagation loss for the six different states. Numerical results show that the cell coverage mainly depends on the none line of sight transmission and the cell average data rate mainly depends on the line of sight transmission.**

***Index Terms*—Communication system performance, millimeter wave communication, radio propagation, fading channels**

I. Introduction

EXPLOSIVE growth of mobile data is imposing great challenges to the design and deployment of future cellular communication networks. To overcome such challenges, researchers have recently shown great interest in the millimeter wave (mmWave) band in the range of 30GHz-300GHz [1]–[4]. Recent measurements in the New York City at 28GHz and 73GHz [5]–[7] shown that the path loss model in mmWave band is comprised of three transmission states, i.e., *Outage* state, *Line of Sight* (LoS) state and *None Line of Sight* (NLoS) state. For the LoS state, no obstruction is located between the transmitter and receiver. For the NLoS state, there are small obstructions such as foliage, building edges, vehicles, and/or pedestrians between the transmitter and receiver [7]. As for the Outage state, there is no link between the transmitter and receiver—that is, the path loss is infinite [5]. As compared to the microwave transmission links which are either in LoS or NLoS state [8], mmWave transmission links are more vulnerable to blockages [9]. Besides, Friis's law states that the radio signals decay exponentially with the carrier frequency, which leads to more severe attenuation loss for the mmWave signals as compared to that for the traditional microwave signals. Results in [10] reveal that the mmWave signals suffer from poorer diffraction, more severe attenuation and lower delay spread, which make the system modelling method of mmWave networks fundamentally different from that of the traditional microwave ones.

The distribution of the propagation loss plays important role for the performances analyses of cellular communication networks [11]. As for traditional microwave, the distribution of the propagation loss including the distance-dependent path loss and shadowing with uniformly distributed users in the circular cell has been analyzed in [12]–[15]. The distributions of the propagation loss for different cell shapes [11], [16], [17] and different distributions of users have been studied in [16]. Furthermore, the distribution of the propagation loss including the large-scale fading and small-scale fading is derived in [18]. The sectorized antenna pattern is considered in [19] and the statistical analysis of the large-scale fading shows that the distribution of the large-scale fading is fully determined by the ratio of attenuation factor to the standard deviation of shadowing. However, current methods or results for the traditional microwave cannot be directly applied to mmWave cellular communication networks because of its unique Out-LoS-NLoS channel model. For mmWave communication networks, theoretical analysis has been carried out based on stochastic geometry theory in [20], [21]. Locations of base stations (BSs) and user equipments (UEs) are modeled as the Poisson Point Process (PPP), based on which the expressions for the cell coverage and the cell average data rate can be derived. Different schemes of the UE associated with the BSs have been studied in [22]. The LoS/NLoS probability functions are considered in the system performances analyses in [23], [24], and the area spectral efficiency for the dense cellular networks is obtained based on the PPP model. The theoretical analysis based on the PPP model only shows the lower bound [25] for the system performance of mmWave communication networks. Based on the statistical model from the real-world measurements, the system-level simulations in [5] have shown that the mmWave networks can greatly improve the capacity of 4G cellular networks without increasing the cell density.

This work is funded by National Natural Science Foundation of China under grants 61571303, 61571100 and 61631005. Corresponding author is J. Xu.

X. Liu and J.Xu are with the Science and Technology on Microsystem Laboratory, Shanghai Institute of Microsystem and Information Technology (SIMIT), Chinese Academy of Sciences (CAS), Shanghai, 200050, P. R. China, and also with the University of Chinese Academy of Sciences, Beijing 100049, P. R. China (e-mail: xiang.liu@wico.sh, xujing1203@hotmail.com).

Y. Pei is with the Singapore Institute of Technology, Infocomm Technology Cluster, 10 Dover Drive, Singapore, 138683 (e-mail: yiyang.pei@singaporetech.edu.sg).

Y.-C. Liang is with the Center for Intelligent Networking and Communications (CINC), University of Electronic Science and Technology of China (UESTC), Chengdu, 611731, P. R. China (e-mail: liangyc@ieee.org).

This article has been accepted for publication in a future issue of this journal, but has not been fully edited. Content may change prior to final publication. Citation information: DOI 10.1109/TVT.2018.2881318, IEEE Transactions on Vehicular Technology

Usually in cellular communication networks, BS positions are planned rather than randomly deployed [17]. The theoretical analysis for mmWave cellular communication networks with the planned BS is needed.

In this paper, theoretical performances analyses including the cell coverage and the cell average data rate based on the propagation loss model of mmWave cellular communication networks are performed. Due to the piecewise nature of the Out-LoS-NLoS probability functions, the signal transmission is either in one of three transmission states, and the user position is either in one of two position states. Then the analyses for the distribution of the propagation loss can be conducted for the separative six states which are jointly determined by the transmission and position states. The resulting distribution of the propagation loss can then be expressed as a six-state mixture distribution. For each state, the distribution of propagation loss is expressed as the three-fold convolution of the distribution of distance-dependent path loss, the distribution of shadowing and the distribution of small-scale fading. The K-L divergence based Gaussian Approximation (KLD-GA) method is proposed, and the distribution of the propagation loss can be well approximated using a Gaussian function for each state. Moreover, the analytical expression of the K-L divergence is derived to characterize the performance of the Gaussian approximation. Then the distribution of the propagation loss including the large-scale fading and the small-scale fading is approximated via a six-state Gaussian mixture model (GMM). The distribution of the signal-to-noise ratio (SNR) based on the distribution of the propagation loss is obtained. Furthermore, the cell coverage of the networks can be expressed as the sum of error functions of the six different states. The cell average data rate is expressed as the weighted sum of the moments of the propagation loss including the large-scale fading and the small-scale fading for the six different states. Investigations of the system performances of the different states show that the NLoS state plays a more important role than the LoS state in the cell coverage, but the cell average data rate mainly depends on the LoS state. The main contributions of this paper are as follows:

1) The analyses for the distribution of the propagation loss for mmWave communication networks are conducted for the separative six states which are jointly determined by the transmission and position states. Then the analytical separative six-state mixture distribution of the propagation loss including the distance-dependent path loss, shadowing and small-scale fading is derived.
2) The distribution of the propagation loss can be well approximated as using a Gaussian function for each state based on our KLD-GA method. The distribution of the propagation loss including the large-scale fading and the small-scale fading can be well approximated via a six-state Gaussian mixture model. All the results obtained from the proposed KLD-GA method are parameterized expressions, which is more accurate than the numerical results of the traditional least square based Gaussian approximation method.
3) Based on the six-state Gaussian mixture distribution of the propagation loss and SNR, the cell coverage is expressed as the weighted sum of error functions of the different states. The cell average data rate is expressed as the weighted sum of the moments of the propagation loss for the different states.

The paper is organized as follows. The system model and problem formulation are presented in Section II. The analysis and approximation of the distribution of the propagation loss based on K-L divergence are given in Section III. And the analytical expression for the system performance based on the distribution of the propagation loss are presented in Section IV. The numerical results of the six-state GMM are shown in Section V. Finally, some conclusions are drawn in Section VI.

II. System Model and Problem formulation

A. Propagation Loss

In this paper, the cellular networks with the planned BS are considered. The signal transmission link for the mmWave is either in one of three transmission states [5], namely, the Line of Sight (LoS) state, None Line of Sight (NLoS) state and Outage state. The link between the UEs and the BS may be blocked by buildings, trees or other obstacles. The blockages of the link result in the *NLoS* state and *Outage* state. The propagation loss of the NLoS state is more severe than that of LoS state. For the Outage state, the propagation loss is so high that the receiver cannot communicate with the transmitter.

In this paper, the polar coordinate system is adopted. We consider that in each cell the BS is located at the origin as shown in Fig. 1. Denote the position of a UE as (r, θ).

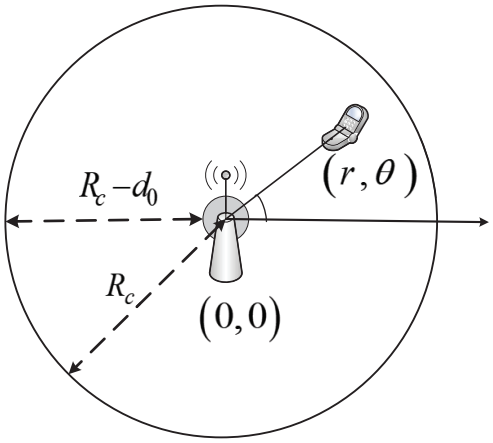

Fig. 1. Cell layout geometry.

Let L_r represent the propagation loss with the position r and it can be expressed as

$$L_r = \begin{cases} L_{1,r}, & \text{with probability } P_1(r) \\ L_{2,r}, & \text{with probability } P_2(r) \\ L_{3,r}, & \text{with probability } P_3(r), \end{cases} \tag{1}$$

where $P_n(r)$ denotes the probability that a user with position r is in transmission state n where $n = 1, 2, 3$ represent the Outage state, LoS state and NLoS state, respectively.

This article has been accepted for publication in a future issue of this journal, but has not been fully edited. Content may change prior to final publication. Citation information: DOI 10.1109/TVT.2018.2881318, IEEE Transactions on Vehicular Technology

Let N represent the random variable of the transmission state, R represent the random variable of the user position, and $L_{n,r}$ represent the propagation loss in dB given the transmission state $N=n$ and the user position $R=r$. Note that $L_{n,r}$ accounts for the effects of both the large-scale fading and small-scale fading and hence it can be expressed as

$$L_{n,r} = Y_{n,r} + Z_{n,r}, n = 1,\ 2,\ 3, \tag{2}$$

where $Y_{n,r}$ and $Z_{n,r}$ denote the large-scale fading and the small-scale fading given the transmission state $N=n$ and the user position $R=r$, respectively. Furthermore, The large-scale fading $Y_{n,r}$ can be expressed as

$$Y_{n,r} = X_{n,r} + S_{n,r}, n = 1,\ 2,\ 3, \tag{3}$$

where $X_{n,r} = \alpha_n + \frac{10\beta_n}{\ln 10}\ln r$ is the distance-dependent path loss given the transmission state $N=n$ and user position $R=r$, α_n and β_n represent the distance-dependent path loss at the reference distance and attenuation factor given the transmission state $N=n$, respectively. $S_{n,r}$ is the shadowing given $N=n$ and $R=r$.

For notational convenience, we denote the distribution of $X_{n,r}$ as $f_{X|N,R}(x|n,r)$, which can be expressed as

$$\begin{aligned} f_{X|N,R}(x|n,r) &\triangleq f_{X|N,R}(x|N=n,R=r) \\ &= \begin{cases} \delta(x-Q), Q\to+\infty; n=1 \\ \delta(x-\alpha_n-10\beta_n \lg r); n=2,3, \end{cases} \end{aligned} \tag{4}$$

where $\delta(\cdot)$ is Dirac delta function. For the Outage state with $n=1$, the distance-dependent path loss is infinite.

It is assumed that shadowing in dB is a Gaussian distributed random variable with zero mean and standard deviation σ_{S_n}, $n=1,\ 2,\ 3$ [5]. Let $f_{S|N,R}(s|n,r)$ denote the distribution of $S_{n,r}$. Given the transmission state, the standard deviation σ_{S_n} of shadowing is assumed to be constant-value, which is independent of the user location [5], [26]. Then, we have

$$\begin{aligned} f_{S|N}(s|n) &= \frac{\int_r f_{S|N,R}(s|n,r) f_{N|R}(n|r) f_R(r)\,dr}{\int_r f_{N|R}(n|r) f_R(r)\,dr} \\ &= f_{S|N,R}(s|n,r) \\ &= \frac{1}{\sqrt{2\pi\sigma_{S_n}^2}} \exp\left(-\frac{s^2}{2\sigma_{S_n}^2}\right), n=1,2,3. \end{aligned} \tag{5}$$

where $f_R(r)$ and $f_{N|R}(n|r)$ represent the distribution of R and distribution of N given R, respectively.

Let $f_{Z|N,R}(s|n,r)$ denote the distribution of $Z_{n,r}$. We adopt the same assumption as that in [27], the parameters Ω_n and m_n for the small-scale fading given the transmission state are assumed to be a constant-value, which is independent of the user location. Hence, we have

$$f_{Z|N}(z|n) = f_{Z|N,R}(z|n,r) = f_{\tilde{Z}|N}(\tilde{z}|n)\left|\frac{\partial\tilde{z}}{\partial z}\right|, \tag{6}$$

where $\tilde{z} = \exp\left(\frac{\ln 10}{10}z\right)$ and $f_{\tilde{Z}|N,R}(\tilde{z}|n,r)$ is the Nakagami distribution function, which is given by

$$\begin{aligned} f_{\tilde{Z}|N}(\tilde{z}|n) &= \frac{\tilde{z}^{m_n-1}}{\Gamma(m_n)}\left(\frac{m_n}{\Omega_n}\right)^{m_n}\exp\left(-\frac{m_n\tilde{z}}{\Omega_n}\right); \\ & m_n \geq 0.5, \quad n=1,2,3, \end{aligned} \tag{7}$$

where $\Gamma(\cdot)$ is the Gamma function, i.e., $\Gamma(m_n) = \int_0^{+\infty} t^{m_n-1}\exp(-t)\,dt$, Ω_n is the mean fading power, and m_n represents the distribution parameter given the transmission state $N=n$. Note that for $m_n=1$ the Nakagami distribution reduces to Rayleigh fading, and for $m_n = (K+1)^2/(2K+1)$ the Nakagami distribution is approximately Rice fading with parameter K [27], then the small-scale fading can be well characterized by the Nakagami distribution.

B. Outage-LoS-NLoS Probability

Various kinds of LoS probability models have been obtained from real-world measurements [28], [29]. For the mmWave transmission links, the unique three-state probability functions are obtained from measurements in New York City [5], which is given as,

1) Outage

$$\begin{aligned} P_1(r) &= \max(0, 1-\exp(-a_1 r + b_1)) \\ &= \begin{cases} P_{1,1}(r) = 0, & d_0 \leqslant r \leqslant d_1 = \frac{b_1}{a_1} \\ P_{1,2}(r) = 1 - e^{b_1 - a_1 r}, & d_1 < r \leqslant R_c, \end{cases} \end{aligned} \tag{8}$$

2) LoS

$$P_2(r) = \begin{cases} P_{2,1}(r) = e^{-a_2 r}, & d_0 \leqslant r \leqslant d_1 \\ P_{2,2}(r) = e^{b_1 - (a_1+a_2)r}, & d_1 < r \leqslant R_c, \end{cases} \tag{9}$$

3) NLoS

$$\begin{aligned} &P_3(r) \\ &= \begin{cases} P_{3,1}(r) = 1 - e^{-a_2 r}, & d_0 \leqslant r \leqslant d_1 \\ P_{3,2}(r) = e^{b_1 - a_1 r}\left(1 - e^{-a_2 r}\right), & d_1 < r \leqslant R_c, \end{cases} \end{aligned} \tag{10}$$

where d_0 is the minimum distance between the UE and BS, and R_c represents the radius of the cell. For any given position of the UE, we have

$$\sum_{i=1}^{3} P_i(r) = 1, \tag{11}$$

$$P_i(r) = \sum_{j=1}^{2} P_{i,j}(r), i = 1,2,3. \tag{12}$$

Let M represent the random variable of the position state. Then the user position is either in one of M states, where $M=1$ represents $R \in [d_0, d_1]$, and $M=2$ represents $R \in (d_1, R_c]$. The joint probability of $N=i$ and $M=j$ given the user position $R=r$ is denoted as $P(i,j|r) \triangleq P(N=i, M=j|R=r) = P_{i,j}(r)$. Similarly, we also use the following simplified notations, $P(i|r) \triangleq P(N=i|R=r)$, and $P(i,j) \triangleq P(N=i, M=j)$. Then

This article has been accepted for publication in a future issue of this journal, but has not been fully edited. Content may change prior to final publication. Citation information: DOI 10.1109/TVT.2018.2881318, IEEE Transactions on Vehicular Technology

the distribution of the state N and M given the user position $R = r$ can be expressed as

$$f_{N,M|R}(n,m|r) = \sum_{i=1}^{3}\sum_{j=1}^{2}\delta(n-i)\,\delta(m-j)\,P(i,j|r), \tag{13}$$

$$f_{N|R}(n|r) = \sum_{i=1}^{3}\delta(n-i)\,P(i|r). \tag{14}$$

The signal transmission is either in one of three transmission states, and the user position is either in one of two transmission states based on the piecewise Out-LoS-NLoS probability functions. Then the analyses for the distribution of the propagation loss can be conducted for the separative six states which are jointly determined by the transmission and position states.

C. Problem Formulation

Based on various distribution functions presented in Section II-A and II-B, we are interested in characterizing the distribution of the propagation loss L which includes the distance-dependent path loss, shadowing and small-scale fading. The closed-form expression of such a distribution will be useful in evaluating the cell coverage and the cell average data rate of an mmWave cellular network in Section V.

We assume that UEs are uniformly distributed in the cell. The distribution of the distance from a UE to the BS is expressed as

$$f_R(r) = \frac{2r}{R_c^2 - d_0^2}, d_0 \leqslant r \leqslant R_c. \tag{15}$$

Since the position state is totally determined by the user position, the distribution of the distance-dependent path loss given the propagation state N, the position state M and the user position R is expressed as

$$f_{X|N,M,R}(x|n,m,r) = f_{X|N,R}(x|n,r). \tag{16}$$

Furthermore, the distribution of the distance-dependent path loss given the transmission state and position state can be expressed as

$$\begin{aligned} f_{X|N,M}(x|n,m) &= \frac{f_{X,N,M}(x,n,m)}{f_{N,M}(n,m)} \\ &= \frac{\int_{d_0}^{R_c} f_{X|N,M,R}(x|n,m,r)\, f_{N,M|R}(n,m|r)\, f_R(r)\, dr}{\int_{d_0}^{R_c} f_{N,M|R}(n,m|r)\, f_R(r)\, dr} \\ &= \frac{\int_{d_0}^{R_c} f_{X|N,R}(x|n,r)\, f_{N,M|R}(n,m|r)\, f_R(r)\, dr}{\int_{d_0}^{R_c} f_{N,M|R}(n,m|r)\, f_R(r)\, dr}. \end{aligned} \tag{17}$$

After integration over the position variable R, the distribution of the distance-dependent path loss given the transmission state N and position state M can be calculated. Denote $L_{N,M}$ as the propagation loss given the transmission state N and position state M, and it can be written as

$$L_{N,M} = Y_{N,M} + Z_{N,M}, \tag{18}$$

where $Y_{N,M}$ and $Z_{N,M}$ represent the large-scale fading and the small-scale given N and M, respectively. Moreover, $Y_{N,M}$ is expressed as

$$Y_{N,M} = X_{N,M} + S_{N,M}, \tag{19}$$

where $X_{N,M}$ and $S_{N,M}$ represent the distance-dependent path loss and shadowing given N and M, respectively. Then the distribution of $L_{N,M}$ can be expressed as

$$\begin{aligned} f_{L|N,M}(l|n,m) &= f_{X|N,M}(x|n,m) \otimes f_{S|N,M}(s|n,m) \\ &\quad \otimes f_{Z|N,M}(z|n,m) \\ &= f_{X|N,M}(x|n,m) \otimes f_{S|N}(s|n) \otimes f_{Z|N}(z|n), \end{aligned} \tag{20}$$

where $\otimes$ represents the convolution operation. The distribution of the propagation loss including the distance-dependent path loss, shadowing and small-scale fading can be expressed as

$$f_L(l) = \int_{-\infty}^{+\infty}\int_{-\infty}^{+\infty} f_{L|N,M}(l|n,m)\, f_{N,M}(n,m)\, dn\, dm, \tag{21}$$

where

$$\begin{aligned} f_{N,M}(n,m) &= \int_{d_0}^{R_c} f_{N,M|R}(n,m|r)\, f_R(r)\, dr \\ &= \int_{d_0}^{R_c}\sum_{i=1}^{3}\sum_{j=1}^{2}\delta(n-i)\,\delta(m-j)\,P(i,j|r)\, f_R(r)\, dr. \end{aligned} \tag{22}$$

It is not easy to obtain a closed-form expression for the propagation loss as shown in (21). Even if such a closed-form expression exists, it might be too complicated to use for the characterization of the cell coverage and the cell average data rate of a mmWave cellular networks. In Section III, an approximate closed-form expression for the distribution of the propagation loss is obtained with the KLD-GA method. Then in Section IV, further results including the closed-form expressions of the cell coverage and the cell average data rate for mmWave cellular networks are obtained.

III. Propagation Loss Analysis based on K-L Divergence

In this section, using the proposed K-L divergence based Gaussian Approximation (KLD-GA) method, we will show that the distribution of the propagation loss including the distance-dependent path loss, shadowing and small-scale fading can be approximated via a six-state Gaussian Mixture Model, which is

$$f_L(l) \approx g_L(l) = \sum_{i=1}^{3}\sum_{j=1}^{2} P(i,j)\,\mathcal{N}\left(l;\mu_{L_{i,j}},\sigma_{L_{i,j}}^2\right), \tag{23}$$

where $\mu_{L_{i,j}}$ and $\sigma_{L_{i,j}}^2$ represent the mean and variance for the approximate Gaussian distribution of propagation loss given the state $N = i, M = j, i = 1,2,3, j = 1,2$, respectively. The exact form of the $\mu_{L_{i,j}}$ and $\sigma_{L_{i,j}}^2$ will be shown in this section.

In Section III-A, the distribution of the propagation loss including the distance-dependent path loss, shadowing and small-scale fading is characterized as a six-state mixture distribution. The KLD-GA method is proposed in Section III-B,

This article has been accepted for publication in a future issue of this journal, but has not been fully edited. Content may change prior to final publication. Citation information: DOI 10.1109/TVT.2018.2881318, IEEE Transactions on Vehicular Technology

and the Gaussian approximation results for the distribution of propagation loss including the large-scale fading and small-scale fading given the state $M = 2$ and $N = 1$ are provided as examples in Section III-B and Section III-C. The performance analysis for the Gaussian approximation based on the proposed method is given in Section III-D.

A. Six-state Mixture Distribution of Propagation Loss

According to the analysis as shown in (21) and (22), the distribution of the propagation loss can be expressed as a mixture distribution, which is given by

$$f_L(l) = \sum_{i=1}^{3}\sum_{j=1}^{2} P(i,j)\, f_{L|M,N}(l|i,j), \tag{24}$$

where

$$P(i,j) = \int_{d_0}^{R_c} P(i,j|r)\, f_R(r)\, dr \tag{25}$$

represents the joint probability that a user is in the state $N = i$ and $M = j$.

Then the distribution of the propagation loss including the distance-dependent path loss, shadowing and small-scale fading resulted from different states can be analyzed separately. Based on Baye's theorem, the distribution of the propagation loss given the transmission state N can be expressed as

$$\begin{aligned} f_{L|N}(l|N=2) = &\frac{P(2,1)}{P(2)} \times f_{L|M,N}(l|2,1) \\ &+ \frac{P(2,2)}{P(2)} \times f_{L|N,M}(l|2,2), \end{aligned} \tag{26}$$

where $P(2) = \int_{d_0}^{R_c} P(2|r)\, f_R(r)\, dr = P(2,1) + P(2,2)$. Since the distribution of the propagation loss given the NLoS state $f_{L|N}(l|3)$ has a similar form to $f_{L|N}(l|2)$, without loss of generality, only the analysis of $f_{L|N}(l|2)$ is given in details. The analysis for the state $N = 2$ can be extended easily to the other states $N = 1, 3$.

B. Analysis of Large-scale Fading

In this subsection, the two-step KL-divergence based Gaussian Approximation (KLD-GA) method is proposed for the analysis of the large-scale fading. Combining (3) and (24), the distribution of the large-scale fading can be expressed as

$$f_Y(y) = \sum_{i=1}^{3}\sum_{j=1}^{2} P(i,j)\, f_{Y|N,M}(y|i,j), \tag{27}$$

where

$$f_{Y|N,M}(y|i,j) = f_{X|N,M}(x|i,j) \otimes f_{S|N}(s|i). \tag{28}$$

More specifically, for the users of LoS state in $[d_0, d_1]$, i.e., $N = 2, M = 1$, we have

$$f_{Y|N,M}(y|2,1) = f_{X|N,M}(x|2,1) \otimes f_{S|N}(s|2), \tag{29}$$

where $f_{X|N,M}(x|2,1)$ and $f_{S|N}(s|2)$ represent the distributions of the distance-dependent path loss and shadowing given $N = 2, M = 1$, respectively. Furthermore, we have

$$f_{X|N,M}(x|2,1) = \frac{0.2\beta_2^{-1}\ln 10}{P(2,1)\left(R_c^2 - d_0^2\right)} w_{2,1}(x), \tag{30}$$

$$w_{2,1}(x) = \exp\left(-a_2 e^{\frac{(x-\alpha_2)\ln 10}{10\beta_2}}\right) \exp\left(\frac{(x-\alpha_2)\ln 10}{5\beta_2}\right),$$
$$x \in \left(\alpha_2 + \frac{10\beta_2}{\ln 10}\ln d_0, \alpha_2 + \frac{10\beta_2}{\ln 10}\lg d_1\right). \tag{31}$$

As shown in (28), the expression for the distribution of large-scale fading is too complicated for further analysis. In order to simplify the computation and show the relationships between system parameters, a simpler closed-form expression is needed. To do so, we first extend the feasible region of the distance-dependent path loss to $(-\infty + \infty)$ by defining a new function $\tilde{w}(x)$ to replace the function $w_{2,1}(x)$ in (30)

$$\tilde{w}(x) \triangleq \frac{1}{A} w_{2,1}(x), x \in (-\infty, +\infty), \tag{32}$$

where

$$A = \int_{-\infty}^{+\infty} w_{2,1}(x)\, dx = \frac{10\beta_2}{a_2^2 \ln 10}. \tag{33}$$

Then, we obtain a simpler closed-form approximate expression for $\tilde{w}(x)$, which is given in the following lemma.

Lemma 1: The optimal Gaussian approximation for the distribution $\tilde{w}(x)$ based on K-L divergence [30] is

$$\tilde{w}(x) \approx \tilde{q}(x) = \mathcal{N}\left(x; \mu_0, \sigma_0^2\right), \tag{34}$$

where

$$\begin{cases} \mu_0 = \left(\ln\frac{2}{a_2} - \frac{1}{4}\right)\frac{10\beta_2}{\ln 10} + \alpha_2 \\ \sigma_0^2 = \frac{50\beta_2^2}{(\ln 10)^2} = 0.5\left(\frac{10\beta_2}{\ln 10}\right)^2. \end{cases} \tag{35}$$

Proof: See Appendix A. ■

The K-L divergence from $\tilde{w}(x)$ to the approximate distribution $\tilde{q}(x)$ with mean μ_0 and variance σ_0^2 can be calculated as $KL(\tilde{q}(x) \| \tilde{w}(x)) = 0.0413$, which is a constant value for the various system parameters. The small K-L divergence validates the performance of the approximation. According to (35), μ_0 and σ_0 are approximately equal to the mean and standard deviation of the distance-dependent path loss of the LoS state, respectively. Moreover, the mean and standard deviation are linear functions of $\frac{10\beta_2}{\ln 10}$. Then by replacing $f_{X|N,M}(x|2,1)$ with $\tilde{q}(x)$ in (28), the distribution of the large-scale fading with $R \in (0, +\infty)$ can be expressed as

$$\begin{aligned} \hat{f}_{Y|N,M}(y|2,1) &= \mathcal{N}\left(x; \mu_0, \sigma_0^2\right) \otimes \mathcal{N}\left(s; 0, \sigma_{S_2}^2\right) \\ &= \mathcal{N}\left(y; \mu_0, \sigma_{S_2}^2 + \sigma_0^2\right), \end{aligned} \tag{36}$$

which is a Gaussian function. Then let $q_{2,1}(x) \triangleq A \times \tilde{q}(x), x \in (\alpha_2 + 10\beta_2 \lg d_0, \alpha_2 + 10\beta_2 \lg d_1)$, and replacing $w_{2,1}(x)$ with $q_{2,1}(x)$ in (30), the distribution of the large-scale fading Y given the transmission $N = 2$ and position state $M = 1$ can be approximated as

$$\begin{aligned} \tilde{f}_{Y|N,M}(y|2,1) = &\mathcal{N}\left(y; \mu_0, \sigma_0^2 + \sigma_{S_2}^2\right) \times C \\ &\times \left(\mathrm{erf}(Dy + E_1) - \mathrm{erf}(Dy + E_2)\right), \end{aligned} \tag{37}$$

This article has been accepted for publication in a future issue of this journal, but has not been fully edited. Content may change prior to final publication. Citation information: DOI 10.1109/TVT.2018.2881318, IEEE Transactions on Vehicular Technology

where $C = \frac{\left(R_c^2-d_0^2\right)^{-1}}{a_2^2 P(2,1)}$, $D = -\frac{\sigma_0}{\sigma_{S_2}\sqrt{2\sigma_{S_2}^2+2\sigma_0^2}}$, $E_1 = \frac{\sigma_0^2(\alpha_2+10\beta_2 \lg d_0)-\sigma_{S_2}^2(\mu_0-\alpha_2-10\beta_2 \lg d_0)}{\sigma_{S_2}\sigma_0\sqrt{2\sigma_{S_2}^2+2\sigma_0^2}}$, $E_2 = \frac{\sigma_0^2(\alpha_2+10\beta_2 \lg d_1)-\sigma_{S_2}^2(\mu_0-\alpha_2-10\beta_2 \lg d_1)}{\sigma_{S_2}\sigma_0\sqrt{2\sigma_{S_2}^2+2\sigma_0^2}}$, and $\mathrm{erf}(\cdot)$ represents an error function. The derived expression (37) can be divided into two parts, the first part is a Gaussian function and the second part is a sum of error functions. Compared with (36), it can be found that the variance of the Gaussian function equals to the sum of variance for the shadowing and distance-dependent path loss. The extra error functions are resulted from the incomplete interval of the integration. Let $d_1 \to +\infty$, and $d_0 \to 0$, then the resulting distribution $\tilde{f}_{Y|N,M}(y|2,1)$ becomes a Gaussian function without error functions. Fig. 2

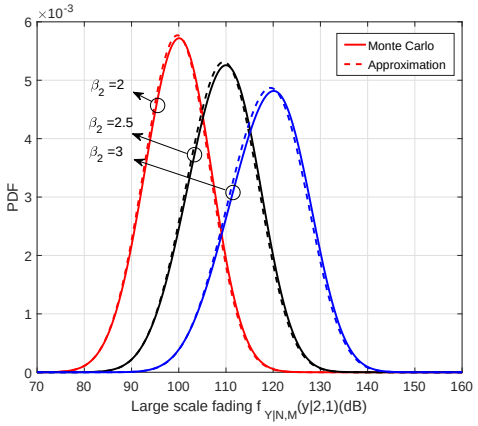

Fig. 2. Distribution of large scale fading given $N = 2, M = 1$ with system parameter $\sigma_{s_2} = 5.8$dB, $a_2 = 1/67.1$, $\alpha_2 = 61.4$dB. Solid lines denote the Monte Carlo simulations. Dashed lines stand for the approximate distributions.

shows the accurate distribution $f_{Y|N,M}(y|2,1)$ and its approximation $\tilde{f}_{Y|N,M}(y|2,1)$ with the system parameters settings according to the results from the real-world measurements [5]. The results in Fig. 2 indicate that the distribution of the large-scale fading can be well approximated using the method proposed above. The performance of the approximation for various system parameters is presented in Section V.

Based on the analysis presented above, the distribution of the distance-dependent path loss plus shadowing is approximated by the Gaussian function multiplied by error functions. Then the cumulant-generating function $K(t)$ of $\tilde{f}_{Y|N,M}(y|2,1)$ can be calculated as

$$K(t) = -\ln\left(\mathrm{erf}\left(-\frac{10\beta_2 \lg d_0-\mu_0}{\sqrt{2\sigma_0^2}}\right)-\mathrm{erf}\left(\frac{10\beta_2 \lg d_1-\mu_0}{\sqrt{2\sigma_0^2}}\right)\right) + \frac{\sigma_0^2+\sigma_{S_2}^2}{2}t^2+(\alpha_2+\mu_0)t + \ln\left(\mathrm{erf}\left(\frac{\sigma_0^2 t-10\beta_2 \lg d_0+\mu_0}{\sqrt{2\sigma_0^2}}\right)-\mathrm{erf}\left(\frac{\sigma_0^2 t-10\beta_2 \lg d_1+\mu_0}{2\sigma_0^2}\right)\right). \quad (38)$$

The detailed proof of (38) is given in Appendix B. Then the n-th normalized cumulants k_n of $\tilde{f}_{Y|N,M}(y|2,1)$ with $\sigma_{s_2} = 5.8$dB, $a_2 = 1/67.1$, $\alpha_2 = 61.4$dB and $\beta_2 = 2$ [5] can be calculated as

$$k_3 = -0.0553,\ k_4 = -0.0648,\ k_5 = 0.0724. \quad (39)$$

Since the higher normalized cumulants of $\tilde{f}_{Y|N,M}(y|2,1)$ approaches zero, $\tilde{f}_{Y|N,M}(y|2,1)$ approaches a Gaussian function. The Gaussian approximation of $\tilde{f}_{Y|N,M}(y|2,1)$ can be obtained based on the following lemma.

Lemma 2: The optimal Gaussian approximation for the distribution of the large-scale fading $Y_{2,1}$ based on the K-L divergence is

$$\tilde{f}_{Y|N,M}(y|2,1) \approx g_{Y|N,M}(y|2,1) = \mathcal{N}\left(y;\mu_{Y_{2,1}},\sigma_{Y_{2,1}}^2\right), \quad (40)$$

where

$$\begin{cases} \mu_{Y_{2,1}} &= \mu_0 - \frac{\sqrt{2\sigma_0^2}}{\sqrt{\pi}}G_{2,1} \\ \sigma_{Y_{2,1}}^2 &= \sigma_0^2+\sigma_{S_2}^2 - \frac{20\sigma_0\beta_2}{\sqrt{2\pi}}F_{2,1} + \frac{2\sigma_0\mu_0}{\sqrt{2\pi}}G_{2,1} - \frac{2\sigma_0^2}{\pi}G_{2,1}^2 \\ G_{2,1} &= \frac{\exp\left(-\frac{(10\beta_2 \lg d_1)^2}{2\sigma_0^2}\right)-\exp\left(-\frac{(10\beta_2 \lg d_0)^2}{2\sigma_0^2}\right)}{\mathrm{erf}\left(\frac{10\beta_2 \lg d_1}{\sqrt{2}\sigma_0}\right)-\mathrm{erf}\left(\frac{10\beta_2 \lg d_0}{\sqrt{2}\sigma_0}\right)} \\ F_{2,1} &= \frac{\lg d_1 \exp\left(-\frac{(10\beta_2 \lg d_1)^2}{2\sigma_0^2}\right)-\lg d_0 \exp\left(-\frac{(10\beta_2 \lg d_0)^2}{2\sigma_0^2}\right)}{\mathrm{erf}\left(\frac{10\beta_2 \lg d_1}{\sqrt{2}\sigma_0}\right)-\mathrm{erf}\left(\frac{10\beta_2 \lg d_0}{\sqrt{2}\sigma_0}\right)}. \end{cases} \quad (41)$$

Proof: See Appendix C. ■

The K-L divergence from $g_{Y|N,M}(y|2,1)$ to $\tilde{f}_{Y|N,M}(y|2,1)$ can be calculated as

$$KL\left(\tilde{f}_{Y|N,M}(y|2,1)\,\|g_{Y|N,M}(y|2,1)\right) = -H(Y_{2,1}) + 0.5\ln 2\pi\sigma_{Y_{2,1}}^2 + 0.5, \quad (42)$$

where $H(Y_{2,1}) \triangleq -\int_{-\infty}^{+\infty}\tilde{f}_{Y|N,M}(y|2,1)\ln\tilde{f}_{Y|N,M}(y|2,1)\,dy$ represents the entropy of $Y_{2,1}$. The performance of the approximation are presented in Section V. The expression for the distribution of the propagation loss for the other states can be derived in a similar manner.

In a summary, first, based on the proposed KLD-GA method, $f_{Y|N,M}(y|i,j)$ can be approximated by a Gaussian function $g_{Y|N,M}(y|i,j) = \mathcal{N}\left(y;\mu_{Y_{i,j}},\sigma_{Y_{i,j}}^2\right)$. Then by replacing $f_{Y|N,M}(y|i,j)$ with $g_{Y|N,M}(y|i,j)$ in (27), we can obtain an approximation for $f_Y(y)$, which is given as the Gaussian mixture distribution function $g_Y(y)$

$$f_Y(y) \approx g_Y(y) = \sum_{i=1}^{3}\sum_{j=1}^{2}P(i,j)\,\mathcal{N}\left(y;\mu_{Y_{i,j}},\sigma_{Y_{i,j}}^2\right). \quad (43)$$

The results of $\mu_{Y_{i,j}},\sigma_{Y_{i,j}}^2, i = 1,3; j = 1,2$ are given in Appendix D.

C. Small-scale Fading

Since Nakagami distribution can be approximated by a log-normal distribution [31], the distribution of Z_i (small scale fading given the transmission state $N = i$) can be approximated by a Gaussian distribution in dB. The approximate mean

This article has been accepted for publication in a future issue of this journal, but has not been fully edited. Content may change prior to final publication. Citation information: DOI 10.1109/TVT.2018.2881318, IEEE Transactions on Vehicular Technology

and standard deviation is expressed as

$$\begin{cases} \mu_{Z_i} & \approx \frac{10}{\ln 10}\left[\psi\left(m_i\right) - \ln m_i\right] \\ \sigma_{Z_i}^2 & \approx \frac{100}{(\ln 10)^2}\varsigma\left(2, m_i\right), \end{cases} \tag{44}$$

where $\psi(\cdot)$ is Euler psi function, $\psi\left(m_i\right) = -C + \sum_{k=1}^{m_{i,j}-1}\frac{1}{k}, C \approx 0.5772$, and $\varsigma\left(2, m_{i,j}\right) = \sum_{k=0}^{+\infty}\frac{1}{(m_{i,j}+k)^2}$ is Riemann's zeta function.

Since the distribution of the large-scale fading and the small-scale fading can be both approximated by Gaussian functions, $f_{L|N,M}\left(l|i,j\right)$ can then be approximated as the convolution of two Gaussian functions. It is easy to verify that $f_{L|N,M}\left(l|i,j\right) \approx g_{L|N,M}\left(l|i,j\right) = \mathcal{N}(l; \mu_{L_{i,j}}, \sigma_{L_{i,j}}^2)$, where $\mu_{L_{i,j}} = \mu_{Y_{i,j}} + \mu_{Z_i}$, $\sigma_{L_{i,j}}^2 = \sigma_{Y_{i,j}}^2 + \sigma_{Z_i}^2$.

Then by replacing $f_{L|N,M}\left(y|i,j\right)$ with $g_{L|N,M}\left(y|i,j\right)$ in (24), the distribution of the propagation loss including the distance-dependent path loss, shadowing and small-scale fading can be approximated as the Gaussian mixture distribution

$$f_L\left(l\right) \approx g_L\left(l\right) = \sum_{i=1}^{3}\sum_{j=1}^{2} P\left(i,j\right)\mathcal{N}\left(l; \mu_{L_{i,j}}, \sigma_{L_{i,j}}^2\right). \tag{45}$$

D. Error Analysis

In the previous section, we have obtained the approximate distribution of the propagation loss based on the proposed KLD-GA method. In this subsection, we will analyze the error of such approximation using K-L divergence. Without loss of generality, we only present the upper bound of the K-L divergence from $f_{L|N,M}\left(l|2,1\right)$ to its approximation as an example, which is given as follows

$$\begin{aligned} &KL\left(g_{L|N,M}\left(l|2,1\right)||f_{L|N,M}\left(l|2,1\right)\right) \leqslant \\ &\quad \ln\frac{P\left(2,1\right)\left(R^2 - d_0^2\right)\sigma_{S_2}}{2\sigma_{L_{21}}\left(d_1+d_0\right)\ln 10} - 0.5 + \frac{a_2\left(d_1-d_0\right)}{\ln d_1 - \ln d_0} \\ &\quad + \frac{\sigma_{L_{2,1}}^2 + \left(\alpha_2 - \mu_{L_{2,1}}\right)^2}{2\sigma_{S_2}^2} + \frac{5\beta_2\left(\alpha_2 - \mu_{L_{21}}\right)}{\sigma_{S_2}^2\ln 10\left(\ln d_1 + \ln d_0\right)^{-1}} \\ &\quad + \frac{50\beta_2^2}{3\sigma_{S_2}^2\ln^2 10}\left(\ln^2 d_1 + \ln d_1 \ln d_0 + \ln^2 d_0\right). \end{aligned} \tag{46}$$

The detail proof is given in Appendix E. According to the upper bound of K-L divergence for the mixture distribution [32], the upper bound of K-L divergence from the distribution of the propagation loss to its approximation can be calculated as

$$\begin{aligned} &KL\left(g_L\left(l\right)||f_L\left(l\right)\right) \leqslant \\ &\quad \sum_{i=1}^{3}\sum_{j=1}^{2} P\left(i,j\right) KL\left(g_{L|N,M}\left(l|i,j\right)||f_{L|N,M}\left(l|i,j\right)\right). \end{aligned} \tag{47}$$

IV. System Performance

In this section, the cell coverage and the cell average data rate in the downlink cellular networks will be analyzed. Firstly, based on the distribution of the propagation loss in Section III, the expressions of the cell coverage for different thresholds and cell radius are obtained. Secondly, an approximation method is introduced to approximate the Shannon's formula and then the cell average data rate based on it is derived, which results in a much simpler form.

A. Cell Coverage

The cell coverage $P_c\left(T\right)$ is defined as the probability that received SNR is larger than the threshold T, i.e., $P_c\left(T\right) \triangleq P\left(SNR > T\right)$. The SNR of a mobile user in the cell can be expressed as

$$SNR = G_t + G_r + P_t - L - P_n, \tag{48}$$

where G_t and G_r represent the gain from the transmitter and the receiver, respectively, P_t is the transmit power, and P_n represents the noise power. Let $G = G_t + G_r + P_t - P_n$. Then the distribution of SNR can be expressed as

$$f_{SNR}\left(w\right) = f_L\left(G - w\right). \tag{49}$$

The cell coverage of the networks can be expressed as the sum of the contributions from the different states,

$$\begin{aligned} P_c\left(T\right) &= P\left(SNR > T\right) = P\left(l < G - T\right) \\ &= P_c^L\left(T\right) + P_c^{NL}\left(T\right) + P_c^O\left(T\right), \end{aligned} \tag{50}$$

where $P_c^L\left(T\right)$ represents the cell coverage of the LoS state contribution, $P_c^{NL}\left(T\right)$ is the cell coverage of the NLoS state contribution, and $P_c^O\left(T\right)$ is the cell coverage of the Outage state contribution, which is equal to 0. Furthermore, $P_c^L\left(T\right)$ and $P_c^{NL}\left(T\right)$ can be expressed as follows

$$\begin{aligned} P_c^L\left(T\right) &= \int_{-\infty}^{G-T} P\left(2\right) \times f_{L|N}\left(l|2\right) dl \\ &\approx \int_{-\infty}^{G-T} P\left(2\right) \times g_{L|N}\left(l|2\right) dl \\ &= \sum_{j=1}^{2}\frac{P\left(2,j\right)}{2}\left(1 + \mathrm{erf}\left(\frac{\mathrm{G-T-\mu_{L_{2,j}}}}{\sigma_{\mathrm{L_{2,j}}}}\right)\right), \end{aligned} \tag{51}$$

$$\begin{aligned} P_c^{NL}\left(T\right) &= \int_{-\infty}^{G-T} P\left(3\right) \times f_{L|N}\left(l|3\right) dl \\ &\approx \int_{-\infty}^{G-T} P\left(3\right) \times g_{L|N}\left(l|3\right) dl \\ &= \sum_{j=1}^{2}\frac{P\left(3,j\right)}{2}\left(1 + \mathrm{erf}\left(\frac{\mathrm{G-T-\mu_{L_{3,j}}}}{\sigma_{\mathrm{L_{3,j}}}}\right)\right). \end{aligned} \tag{52}$$

Note that $P_c^L\left(T\right)$ and $P_c^{NL}\left(T\right)$ are expressed as sums of error functions which are convenient for further calculation and analysis.

B. Cell Average Data Rate

The spectral efficiency can be calculated as

$$\begin{aligned} R &= E\left[\log_2\left(1 + SNR\right)\right] \\ &= \int_{-\infty}^{+\infty}\log_2\left(1 + 10^{\frac{G-l}{10}}\right) f_L\left(l\right) dl. \end{aligned} \tag{53}$$

This article has been accepted for publication in a future issue of this journal, but has not been fully edited. Content may change prior to final publication. Citation information: DOI 10.1109/TVT.2018.2881318, IEEE Transactions on Vehicular Technology

Then we approximate the Shannon's formula $\log_2(1+x)$ using the expansion of the base function $\log_{10}(x)$, which is expressed as

$$f(x) = \log_2(1+x) \approx c_0 + c_1 \log_{10}(x) + c_2 (\log_{10}(x))^2, \quad (54)$$

where the parameter c_0, c_1, c_2 can be obtained by solving the following optimization problem.

$$(c_0, c_1, c_2) = \arg\min_{c_0,c_1,c_2} \int_{-\infty}^{+\infty} \begin{pmatrix} \log_2(1+x) - c_0 \\ -c_1 \log_{10}(x) - c_2 (\log_{10}(x))^2 \end{pmatrix}^2 dx. \quad (55)$$

Using the trust region algorithm [33], the numerical values of c_0, c_1, c_2 can be obtained. By substituting c_0, c_1, c_2 into (53), the approximate cell average data rate can be expressed as

$$\tilde{R} = \int_{-\infty}^{+\infty} \log_2\left(1 + 10^{\frac{G-l}{10}}\right) f_L(l)\, dl \approx \int_{-\infty}^{+\infty} \left(c_0 + c_1 \frac{G-l}{10} + c_2 \left(\frac{G-l}{10}\right)^2\right) f_L(l)\, dl. \quad (56)$$

Let $e_0 \triangleq c_0 + c_1 \frac{G}{10}$, $e_1 \triangleq \frac{5c_1 + c_2 G}{50}$, and $e_2 \triangleq \frac{c_2}{100}$, then the cell average data rate as shown in (56) can be rewritten as

$$\tilde{R} = \sum_{i=1}^{3}\sum_{j=1}^{2} P(i,j)\left(e_0 - e_1 \mu_{L_{i,j}} + e_2\left(\mu_{L_{i,j}}^2 + \sigma_{L_{i,j}}^2\right)\right) = \tilde{R}_L + \tilde{R}_{NL} + R_O. \quad (57)$$

where

$$\tilde{R}_L = \sum_{j=1}^{2} P(2,j)\left(e_0 - e_1 \mu_{L_{2,j}} + e_2\left(\mu_{L_{2,j}}^2 + \sigma_{L_{2,j}}^2\right)\right), \quad (58)$$

$$\tilde{R}_{NL} = \sum_{j=1}^{2} P(3,j)\left(e_0 - e_1 \mu_{L_{3,j}} + e_2\left(\mu_{L_{3,j}}^2 + \sigma_{L_{3,j}}^2\right)\right). \quad (59)$$

As shown in (57), the cell average data rate can be approximated as a weighted sum of the first and the second order raw moment of the distribution of the propagation loss for the different states. Since the users in the Outage state cannot communicate with the BS, the cell average data rate contribution from the Outage state equals 0, i.e., $R_O = 0$. The fractions of the LoS and NLoS contribution can be defined as

$$\eta_L^{Rate} = \frac{\tilde{R}_L}{\tilde{R}}, \quad (60)$$

$$\eta_{NL}^{Rate} = \frac{\tilde{R}_{NL}}{\tilde{R}}, \quad (61)$$

it can be verified that $\eta_L^{Rate} + \eta_{NL}^{Rate} \equiv 1$.

V. Numerical Results

In this section, the performance of the theoretical analysis is verified using numerical results. The system parameters [5] are given in Table I.

TABLE I
Setting of System Parameters

System Parameter	Value
Carrier frequency	28GHz
Cell radius	30∼400m
Minimum distance between UEs and the BS	30m
Path loss at the reference distance for LoS / NLoS	61.4dB / 72dB
Attenuation factor for LoS / NLoS	2 / 2.92
Standard deviation for shadowing of LoS / NLoS	5.8dB / 8.7dB
Outage-LoS-NLoS probability parameters setting	$1/a_1$ = 30.0m b_1 = 5.2 $1/a_2$ = 67.1m

A. Distribution of Propagation Loss for Each Transmission State

In this subsection, the performances of the approximate distribution of the propagation loss including the large-scale fading and small-scale fading for each transmission state based on the proposed KLD-GA method are investigated.

We first verify the performance of the proposed approximate distribution of the large-scale fading of the LoS state of users' position in $[d_0, d_1]$ depicted in Fig. 3 as an example. It is observed that the approximate results perfectly match those of Monte Carlo simulations. Furthermore, with the increase of standard deviation of the shadowing, the accuracy of the approximation improves. Compared with the Least Square based Gaussian Approximation (LS-GA) method, the approximate distributions based on the KLD-GA method are closer to the results of Monte Carlo simulations, especially in the tail of the distributions.

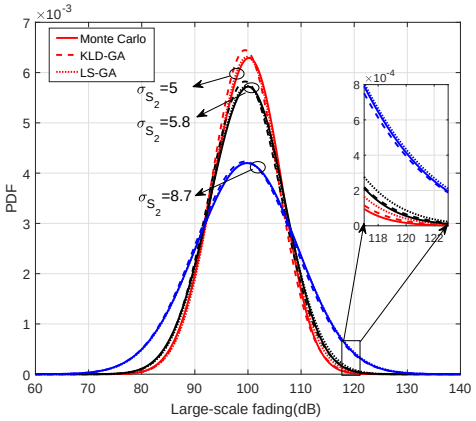

Fig. 3. Distribution of the large-scale fading and its approximations based on the KLD-GA method and LS-GA method given $N = 2, M = 1$. Solid lines denote the Monte Carlo simulations. Dashed lines stand for the approximate distributions based on the KLD-GA method. Dotted lines stand for the approximate distributions based on the LS-GA method.

Next, we show the K-L divergences from the distributions of the Monte Carlo simulations to the approximate distributions under different settings of the standard deviations of shadowing and the attenuation factors in Table II and Table III. It is observed in Table II that for different standard deviations of shadowing, the approximate distributions based on the KLD-GA method always result in smaller K-L divergences than those based on the LS-GA method. This shows that our

This article has been accepted for publication in a future issue of this journal, but has not been fully edited. Content may change prior to final publication. Citation information: DOI 10.1109/TVT.2018.2881318, IEEE Transactions on Vehicular Technology

approximation has better accuracy. Similar observation can be made when we vary the attenuation factors, as shown in Table III. Furthermore, the results in Table II and Table III indicate that the performance of the approximations based on those two methods improves with the increase in the standard deviation of shadowing or the decrease in the attenuation factor.

TABLE II
PERFORMANCE COMPARISON OF THE KLD-GA METHOD AND THE LS-GA METHOD IN TERMS OF STANDARD DEVIATIONS OF SHADOWING

Parameter Setting	K-L Divergence	
	KLD-GA	LS-GA
$\sigma_{S_2} = 5.0,\ \beta_2 = 2$	0.002017	0.05884
$\sigma_{S_2} = 5.8,\ \beta_2 = 2$	0.001216	0.003474
$\sigma_{S_2} = 8.7,\ \beta_2 = 2$	0.0003657	0.0007722

TABLE III
PERFORMANCE COMPARISON OF THE KLD-GA METHOD AND THE LS-GA METHOD IN TERMS OF ATTENUATION FACTORS

Parameter Setting	K-L Divergence	
	KLD-GA	LS-GA
$\beta_2 = 2.0,\ \sigma_{S_2} = 5.8$	0.001216	0.003474
$\beta_2 = 2.5,\ \sigma_{S_2} = 5.8$	0.002620	0.007625
$\beta_2 = 3.0,\ \sigma_{S_2} = 5.8$	0.004965	0.01405
$\beta_2 = 3.5,\ \sigma_{S_2} = 5.8$	0.008363	0.02296

In Fig. 4, the results of Monte Carlo simulations and its approximate distributions of the propagation loss including the large-scale fading and the small-scale fading for the different parameters are illustrated. K factors of the Rice distributions for the small-scale fading are obtained from the real world measurements [34]. The approximate distributions based on the KLD-GA method match well with the results of the Monte Carlo simulations, especially in the tail of the distributions. The K-L divergences from the results of Monte Carlo simulations to the approximate distributions are presented in Table IV. The K-L divergences of the results for the KLD-GA method are less than that of the results based on the LS-GA method. This indicates that the approximate distributions of the propagation loss including the large-scale fading and the small-scale fading based on the KLD-GA method are more accurate than the results based on the LS-GA method in terms of K factors.

B. Distribution of Propagation Loss

In this subsection, the distribution of the propagation loss including the large-scale fading and the small-scale fading are illustrated. The distribution of the propagation loss including the distance-dependent path loss, shadowing and small-scale fading can be expressed as the convolution of the distributions of those three components. According to the analysis in Section III, the distribution of the propagation loss for each transmission state and position state can be approximated as the sum of the Gaussian functions. Therefore, the distribution for the sum of the all states can be approximated via Gaussian

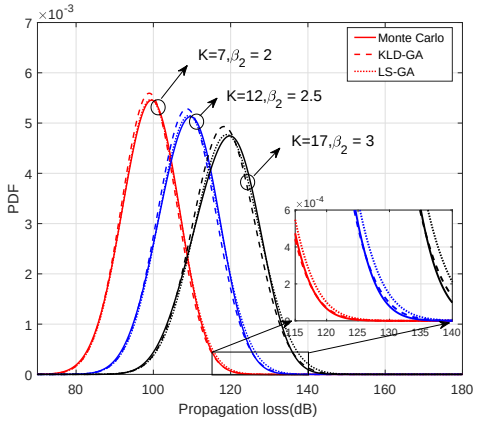

Fig. 4. Distribution of the propagation loss and its approximations including the large-scale fading and the small-scale fading. Solid lines denote the Monte Carlo simulations. Dashed lines stand for the approximate distributions based on the KLD-GA method. Dotted lines stand for the approximate distributions based on the LS-GA method.

TABLE IV
PERFORMANCE COMPARISON OF THE KLD-GA METHOD AND THE LS-GA METHOD FOR THE DIFFERENT K FACTOR

Parameter Setting	K-L Divergence	
	KLD-GA	LS-GA
$K = 7,\ \beta_2 = 2.00,\ \sigma_{S_2} = 5.8$	0.0014	0.0029
$K = 12,\ \beta_2 = 2.00,\ \sigma_{S_2} = 5.8$	0.0012	0.0031
$K = 17,\ \beta_2 = 2.00,\ \sigma_{S_2} = 5.8$	0.0012	0.0032
$K = 7,\ \beta_2 = 2.92,\ \sigma_{S_2} = 8.7$	0.0012	0.0029
$K = 12,\ \beta_2 = 2.92,\ \sigma_{S_2} = 8.7$	0.0011	0.0030
$K = 17,\ \beta_2 = 2.92,\ \sigma_{S_2} = 8.7$	0.0011	0.0030

mixture model. As shown in Fig. 5, the approximate distributions perfectly match with the results of the Monte Carlo simulations.

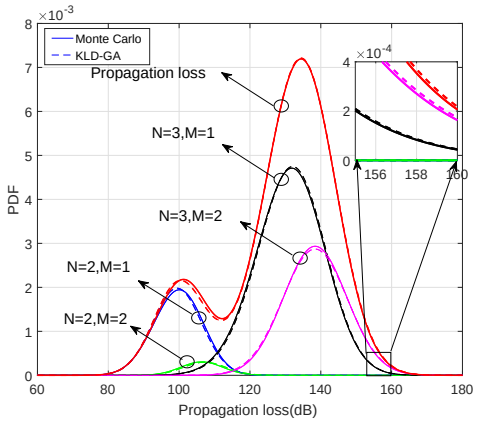

Fig. 5. The performance of the KLD-GA method for each state and the approximate distribution of the propagation loss based on the Gaussian mixture model. Solid lines denote the Monte Carlo simulations. Dashed lines stand for the approximate distributions based on the KLD-GA method.

This article has been accepted for publication in a future issue of this journal, but has not been fully edited. Content may change prior to final publication. Citation information: DOI 10.1109/TVT.2018.2881318, IEEE Transactions on Vehicular Technology

C. System Performance

In this subsection, numerical results of the cell coverage and the cell average data rate based on the proposed KLD-GA method are presented. In Fig. 6, the cell coverage of mmWave networks for different cell radii at different SNR thresholds are depicted. The approximate results perfectly match with the results of the Monte Carlo simulations.

In Fig. 7, the cell coverage for the contributions of different transmission states are presented. The fractions of the contributions for different transmission states are shown in Fig. 7(b). The results in Fig. 7(a) show that the cell coverage for different radii can be divided into three stages. When the cell radius is in the interval of $(30, 62]$m, the cell coverage of the LoS contribution is larger than that of the NLoS contribution. When the cell radius is in $(62, 156]$m, the cell coverage decreases slowly with the increase of the cell radius. The cell coverage of the NLoS contribution increases with the cell radius. The NLoS contribution is larger than the LoS contribution. When the cell radius is larger than 156m, the NLoS contribution decreases with the cell radius. The fraction of the NLoS contribution, in this case, is larger than that of the LoS contribution and it accounts for more than 73.6% of the cell coverage as shown in Fig. 7(b). When the cell radius gets larger, the probability of the Outage state increases dramatically, the cell coverage decreases accordingly.

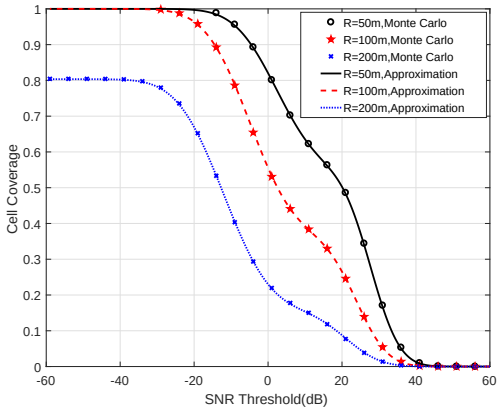

Fig. 6. Cell Coverage of different threshold for various of cell radii, with $P_t = 30$ dBm, Noise Figure=10 dB, $B_w = 2$ GHz, $G_t = 20, G_r = 0$ dB.

The cell average rate of mmWave networks compared with microwave networks are presented in Table V. The system settings of the C2 environment of WINNER II channel model [8] are adopted for the microwave networks. The bandwidths of the mmWave networks and the microwave networks are set as 2GHz and 40MHz, respectively. Due to the smaller wavelength of the mmWave, there is an extra 20dB gain from BS antenna for the mmWave networks. In our simulation, 64QAM is adopted for the modulation scheme. Hence, the maximum spectral efficiency for the microwave networks is 6bps/Hz. As shown in Table V, the cell average spectral efficiency of the mmWave networks is smaller than that of the microwave networks. However, due to the larger bandwidth, more than 10 times of the cell average data rate can be provided by the mmWave networks. For the cell edge users, the mmWave

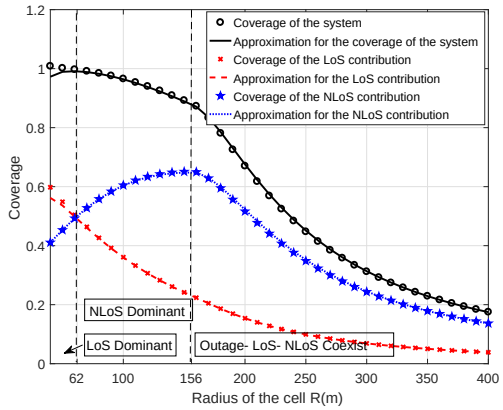

(a) The cell coverage for threshold equals to -20dB versus cell radii.

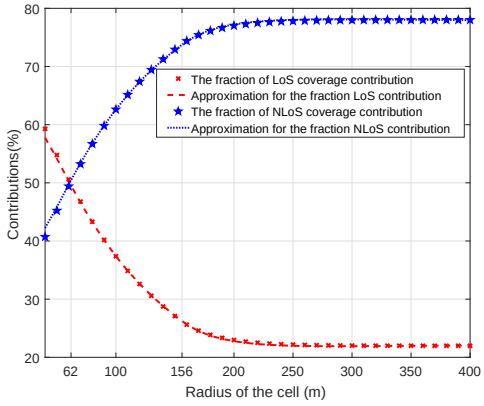

(b) The fractions of the cell coverage for the contributions of different transmission states.

Fig. 7. The cell coverage for the contributions of different transmission states.

networks can offer an comparable cell average data rate to the microwave networks when cell radius is smaller than 50m. Due to the severe loss of mmWave signals for the long-distance transmissions, the data rate of edge users of mmWave networks for the radius of 200m and 400m are extremely small. In Fig. 8, we compare the Shannon's formula with the proposed approximation based on the second-order series expansion. The coefficients in the proposed approximation are obtained based on the least square (LS) fitting method.

The approximate result obtained from LS fitting method perfectly matches the accurate Shannon's formula with an R-square value of 0.9986. In Fig. 9(a), the cell average data rate of the mmWave networks is presented. It is observed that the cell average data rate decreases dramatically with the increase in the cell radius. In Fig. 9(b), the fractions of the contributions of different transmission states are illustrated. It is observed that the fraction of the LoS contribution decreases with the increase in cell radius. It can be found that more than eighty percent of the cell average data rate are provided by the LoS contribution ($\frac{\tilde{R}_L}{\tilde{R}} > 80\%$). The cell average data rate of the NLoS contribution is smaller than that of the LoS contribution due to the severe loss of the NLoS links.

This article has been accepted for publication in a future issue of this journal, but has not been fully edited. Content may change prior to final publication. Citation information: DOI 10.1109/TVT.2018.2881318, IEEE Transactions on Vehicular Technology

TABLE V
DATA RATE OF THE MMWAVE AND MICROWAVE NETWORKS

	cell radius (m)	Average Spec. eff (bps/Hz)	Cell Average throughput (Mbps)	5% Cell edge data rate (Mbps)
mmWave	50	5.4287	10857	235.01
	100	3.1134	6226.8	26.740
	200	1.1800	2360.0	0.0023
	400	0.29374	587.47	0.0
microwave	50	5.9189	236.76	238.51
	100	5.1967	207.87	64.0122
	200	3.3498	133.99	6.2441
	400	1.5233	60.933	0.4981

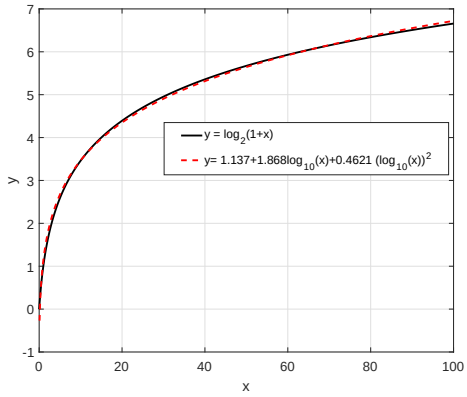

Fig. 8. The approximation of the Shannon's formula based on the LS fittng method.

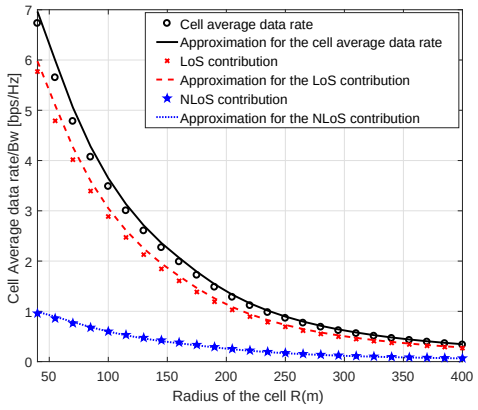

(a) The spectrum efficiency versus cell radii for the LoS/NLoS transmission states.

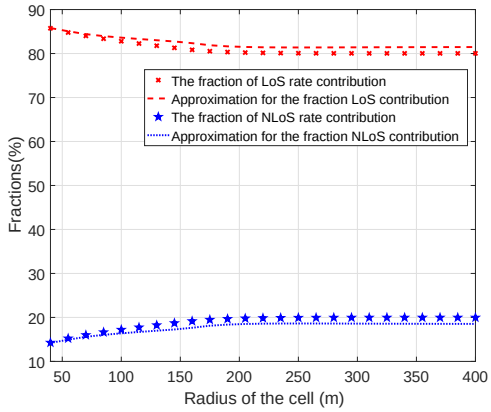

(b) The fractions of spectrum efficiency versus cell radii for LoS/NLoS contributions.

Fig. 9. The spectrum efficiency for the contributions of different transmission states.

Based on the proposed numerical results, we can conclude that cell average data rate of the mmWave networks mainly depends on the LoS transmission while the cell coverage of the mmWave networks mainly depends on the NLoS transmission when cell radius is within $(156, 400]$m.

VI. CONCLUSION

In this paper, the system performances including the cell coverage and the cell average rate for mmWave communication networks are studied. Based on the unique three-state probability functions and the propagation attenuation models from the real-world measurements, we first derived the six-state mixture distribution of the propagation loss including the distance-dependent loss, shadowing and the small-scale fading. We further proposed the K-L divergence based Gaussian Approximation (KLD-GA) method, and the distribution of the propagation loss including the large-scale fading and small-scale fading is approximated via an analytical six-state Gaussian mixture model. Numerical results show that the approximate distribution based on the proposed method is more accurate than the approximate distribution based on the LS-GA method for the different system parameters.

Based on the proposed six-state GMM of the propagation loss and SNR for mmWave communication networks, the cell coverage is expressed as the weighted sum of error functions of the different states, which is shown to be mathematically tractable and also a good fit with the Monte Carlo simulations. Investigations upon the cell coverage for the different states show that the cell coverage are mainly (more than 70%) provided by the NLoS transmission links for a large cell (when the cell radius is larger than 156m). Furthermore, the Shannon's formula is approximated by the the second-order series expansion based on the logarithm function, then the cell average data rate can be expressed as the weighted sum of the moments of the propagation loss for the different states. Numerical results show that the cell average data rate decreases dramatically with the increase of the cell radius due to the severe loss. The cell average data rate of mmWave cellular communication networks mainly (more than 80%)

This article has been accepted for publication in a future issue of this journal, but has not been fully edited. Content may change prior to final publication. Citation information: DOI 10.1109/TVT.2018.2881318, IEEE Transactions on Vehicular Technology

depends on the LoS transmission.

APPENDIX A
PROOF OF LEMMA 1

The optimal Gaussian approximation of $p(x)$ can be obtained by solving the optimization problem

$$\left(\mu_0, \sigma_0^2\right) = \arg\min_{\mu,\sigma^2} \left\{ KL\left(q\left(x\right) \| p\left(x\right)\right)\right\}. \tag{62}$$

The K-L divergence can be calculated as

$$\begin{aligned} KL\left(q\left(x\right)||p\left(x\right)\right) = &-\frac{1}{2}\ln 2\pi\sigma^2 + \ln A - \frac{\mu \ln 10}{5\beta_2} \\ &- \frac{1}{2} + a_2 \exp\left(\mu\frac{\ln 10}{10\beta_2} + \frac{\sigma^2\left(\ln 10\right)}{200\beta_2^2}\right). \end{aligned} \tag{63}$$

According to the optimization theory, the stable point can be calculated by

$$\begin{cases} \left.\frac{\partial KL}{\partial \mu}\right|_{\mu=\mu_0} = 0 \\ \left.\frac{\partial KL}{\partial (\sigma^2)}\right|_{\sigma^2=\sigma_0^2} = 0 \end{cases} \Rightarrow \begin{cases} \mu_0 = \left(\ln\frac{2}{a_2} - \frac{1}{4}\right)\frac{10\beta_2}{\ln 10} + \alpha_2 \\ \sigma_0^2 = \frac{50\beta_2^2}{\left(\ln 10\right)^2} = 0.5\left(\frac{10\beta_2}{\ln 10}\right)^2, \end{cases} \tag{64}$$

The K-L divergence from $p(x)$ to $q(x)$ is $KL\left(q\left(x\right)||p\left(x\right)\right)|_{q(x)=\mathcal{N}\left(x;\mu_0,\sigma_0^2\right)} = 0.0413$. Furthermore, by calculating the first order and the second order derivative of $KL\left(q\left(x\right)||p\left(x\right)\right)$, it is easy to verify that the Hessian matrix of $KL\left(q\left(x\right)||p\left(x\right)\right)$ is positive definite,

$$\left.\frac{\partial^2 KL\left(q\|p\right)}{\partial\mu^2}\right|_{\mu_0,\sigma_0^2} = a_{LoS}\left(\frac{\ln 10}{10\beta_2}\right)^2 e^{\mu_0\frac{\ln 10}{10\beta_2} + \frac{{\sigma_0}^2(10)^2}{200\beta_2^2}} > 0, \tag{65}$$

$$\begin{aligned} &\left|\begin{matrix} \frac{\partial^2 KL(q\|p)}{\partial\mu^2} & \frac{\partial^2 KL(q_{21}\|p_{21})}{\partial\mu\partial(\sigma^2)} \\ \frac{\partial^2 KL(q\|p)}{\partial(\sigma^2)\partial\mu} & \frac{\partial^2 KL(q_{21}\|p_{21})}{\partial(\sigma^2)^2} \end{matrix}\right|_{\mu=\mu_0,\sigma^2=\sigma_0^2} \\ &= \frac{a_2}{2\sigma_0^4} e^{\frac{\mu_0\ln 10}{10\beta_2} + \frac{\sigma_0^2(\ln 10)^2}{200\beta_2^2}} \left(\frac{\ln 10}{10\beta_2}\right)^2 > 0. \end{aligned} \tag{66}$$

Then the solution of optimization problem (62) is $\left(\mu_0, \sigma^2\right)$. Then we get the optimal Gaussian approximation based on the K-L divergence.

APPENDIX B
PROOF OF (38)

According to the analytical expression as shown in (37), the approximation for the distribution of $Y_{2,1}$ is expressed as

$$\begin{aligned} &\tilde{f}_{Y|N,M}\left(y|2,1\right) \\ &= \tilde{A}\int_{\alpha_2+10\beta_2\frac{\ln d_0}{\ln 10}}^{\alpha_2+10\beta_2\frac{\ln d_1}{\ln 10}} \frac{e^{-\frac{(y-x)^2}{2\sigma_{S_2}^2}}}{\sqrt{2\pi\sigma_{S_2}^2}} \frac{e^{\frac{-(x-\mu_0)^2}{2\sigma_0^2}}}{\sqrt{2\pi\sigma_0^2}} dx, \end{aligned} \tag{67}$$

where

$$\tilde{A} = \frac{2}{\left(\mathrm{erf}\left(-\frac{10\beta_2\lg d_0 - \mu_0}{\sqrt{2\sigma_0^2}}\right) - \mathrm{erf}\left(-\frac{10\beta_2\lg d_1 - \mu_0}{\sqrt{2\sigma_0^2}}\right)\right)}. \tag{68}$$

Then the moment-generating function of $\tilde{f}_{Y|N,M}\left(y|2,1\right)$ can be calculated as

$$\begin{aligned} M_{Y_{21}}\left(t\right) &= \int_{-\infty}^{+\infty} \tilde{f}_{Y|N,M}\left(y|2,1\right) e^{ty} dy \\ &= \frac{\tilde{A}}{2}\exp\left(\frac{\sigma_0^2}{2}t^2\right)\left(\begin{matrix} \mathrm{erf}\left(\frac{\sigma_0^2 t - 10\beta_2\lg d_0 + \mu_0}{\sqrt{2\sigma_0^2}}\right) \\ -\mathrm{erf}\left(\frac{\sigma_0^2 t - 10\beta_2\lg d_1 + \mu_0}{\sqrt{2\sigma_0^2}}\right) \end{matrix}\right) \\ &\times \exp\left(\frac{\sigma_{S_2}^2 t^2}{2} + \left(\alpha_2 + \mu_0\right)t\right). \end{aligned} \tag{69}$$

The cumulant-generating function $K\left(t\right)$ of $\tilde{f}_{Y_{2,1}}\left(y\right)$ can be calculated as

$$K\left(t\right) = \ln M_{Y_{2,1}}\left(t\right), \tag{70}$$

then the result as shown in (38) is obtained.

APPENDIX C
PROOF OF LEMMA 2

Let $g_{Y_{2,1}}\left(y\right) = \mathcal{N}\left(\mu, \sigma^2\right)$. The optimal Gaussian approximation of $\tilde{f}_{Y_{2,1}}\left(y\right)$ can be obtained by solving the optimization problem

$$\begin{aligned} &\left(\mu_{Y_{2,1}}, \sigma_{Y_{2,1}}^2\right) \\ &= \arg\min_{\mu,\sigma^2}\left\{KL\left(\tilde{f}_{Y|N,M}\left(y|2,1\right)\|g_{Y|N,M}\left(y|2,1\right)\right)\right\}. \end{aligned} \tag{71}$$

According to the definition of K-L divergence, we have

$$\begin{aligned} &KL\left(\tilde{f}_{Y|N,M}\left(y|2,1\right)\|g_{Y|N,M}\left(y|2,1\right)\right) \\ &= \int_{-\infty}^{+\infty} \tilde{f}_{Y|N,M}\left(y|2,1\right)\ln\tilde{f}_{Y|N,M}\left(y|2,1\right)dy \\ &- \int_{-\infty}^{+\infty} \tilde{f}_{Y|N,M}\left(y|2,1\right)\ln g_{Y|N,M}\left(y|2,1\right)dy. \end{aligned} \tag{72}$$

According to the optimization theory, we have

$$\begin{aligned} &\begin{cases} \left.\frac{\partial\left\{KL\left(\tilde{f}_{Y|N,M}(y|2,1)\|g_{Y|N,M}(y|2,1)\right)\right\}}{\partial\mu}\right|_{\mu=\mu_{Y_{2,1}}} = 0 \\ \left.\frac{\partial\left\{KL\left(\tilde{f}_{Y|N,M}(y|2,1)\|g_{Y|N,M}(y|2,1)\right)\right\}}{\partial\sigma^2}\right|_{\sigma^2=\sigma_{Y_{2,1}^2}} = 0 \end{cases} \\ &\Rightarrow \begin{cases} \mu_{Y_{2,1}} = \mu_{\tilde{f}_{Y_{2,1}}} \\ \sigma_{Y_{2,1}}^2 = \sigma_{\tilde{f}_{Y_{2,1}}}^2. \end{cases} \end{aligned} \tag{73}$$

where

$$\mu_{\tilde{f}_{Y_{2,1}}} = \mu_0 - \frac{\sqrt{2\sigma_0^2}}{\sqrt{\pi}}G_{2,1}, \tag{74}$$

$$\begin{aligned} \sigma_{\tilde{f}_{Y_{2,1}}}^2 = &\sigma_0^2 + \sigma_{s_2}^2 - \frac{2\sigma_0 10\beta_2}{\sqrt{2\pi}}F_{2,1} + \frac{2\sigma_0\mu_0}{\sqrt{2\pi}}G_{2,1} \\ &- \frac{2\sigma_0^2}{\pi}G_{2,1}^2, \end{aligned} \tag{75}$$

This article has been accepted for publication in a future issue of this journal, but has not been fully edited. Content may change prior to final publication. Citation information: DOI 10.1109/TVT.2018.2881318, IEEE Transactions on Vehicular Technology

$$G_{2,1}=\frac{\exp\left(-\frac{(10\beta_2\lg d_1)^2}{2\sigma_0^2}\right)-\exp\left(-\frac{(10\beta_2\lg d_0)^2}{2\sigma_0^2}\right)}{\mathrm{erf}\left(\frac{10\beta_2\lg d_1}{\sqrt{2}\sigma_0}\right)-\mathrm{erf}\left(\frac{10\beta_2\lg d_0}{\sqrt{2}\sigma_0}\right)}, \tag{76}$$

$$F_{2,1}=\frac{\lg d_1\exp\left(-\frac{(10\beta_2\lg d_1)^2}{2\sigma_0^2}\right)-\lg d_0\exp\left(-\frac{(10\beta_2\lg d_0)^2}{2\sigma_0^2}\right)}{\mathrm{erf}\left(\frac{10\beta_2\lg d_1}{\sqrt{2}\sigma_0}\right)-\mathrm{erf}\left(\frac{10\beta_2\lg d_0}{\sqrt{2}\sigma_0}\right)}. \tag{77}$$

Its Hessian matrix is positive definite

$$\left[\begin{array}{cc}\frac{\partial^2 KL'}{\partial\mu^2} & \frac{\partial^2 KL'}{\partial\mu\partial\sigma^2}\\ \frac{\partial^2 KL'}{\partial\sigma^2\partial\mu} & \frac{\partial^2 KL'}{\partial(\sigma^2)^2}\end{array}\right]_{\mu=\mu_{L_{2,1}},\sigma^2=\sigma^2_{L_{2,1}}}\succ 0. \tag{78}$$

where $KL'=KL\left(\tilde{f}_{Y|N,M}\left(y|2,1\right)\|g_{Y|N,M}\left(y|2,1\right)\right)$. Hence, the optimization problem (71) can be solved and the solution is shown in (41). The minimum K-L divergence can be calculated as

$$\begin{aligned}&KL\left(\tilde{f}_{Y|N,M}\left(y|2,1\right)\|g_{Y|N,M}\left(y|2,1\right)\right)\\&=-H\left(Y_{2,1}\right)+0.5\ln 2\pi\sigma^2_{Y_{2,1}}+0.5,\end{aligned} \tag{79}$$

where $H\left(Y_{2,1}\right)$ represents the entropy of $Y_{2,1}$.

Appendix D
Results for the Outage state and NLoS state

1) Outage state $n=1,m=1$,

$$\begin{cases}\mu_{Y_{1,1}} &= M, M\to+\infty\\ \sigma^2_{Y_{1,1}} &= \sigma^2_{S_1}\\ P\left(1,1\right) &= 0.\end{cases} \tag{80}$$

2) Outage state $n=1,m=2$,

$$\begin{cases}\mu_{Y_{1,2}} &= M, M\to+\infty\\ \sigma^2_{Y_{1,2}} &= \sigma^2_{S_1}\\ P\left(1,2\right) &= \frac{R_c^2-d_1^2}{R_c^2-d_0^2}+2\frac{2R_ce^{-a_1R_c+b_1}}{a_1\left(R_c^2-d_0^2\right)}-2\frac{d_1e^{-a_1d_1+b_1}}{a_1\left(R_c^2-d_0^2\right)}\\ &\quad+2\frac{e^{-a_1R_c+b_1}}{a_1\left(R_c^2-d_0^2\right)}-2\frac{e^{-a_1d_1+b_1}}{a_1^2\left(R_c^2-d_0^2\right)}.\end{cases} \tag{81}$$

3) NLoS state $n=3,m=1$,

$$\begin{cases}\mu_{Y_{3,1}} &= P_1\left(3,1\right)\mu_{3,1,1}-P_2\left(3,1\right)\mu_{3,1,2}\\ \sigma^2_{Y_{3,1}} &= \mu^2_{Y_{3,1}}+P_1\left(3,1\right)\left(\sigma^2_{3,1,1}-\mu^2_{3,1,1}\right)\\ &\quad-P_2\left(3,1\right)\left(\sigma^2_{3,1,2}-\mu^2_{3,1,2}\right)\\ P\left(3,1\right) &= P_1\left(3,1\right)-P_2\left(3,1\right),\end{cases} \tag{82}$$

where

$$\begin{cases}\mu_{3,1,1} &= \alpha_3-\frac{5\beta_3}{\ln 10}+10\beta_3M_{3,1,1}\\ \sigma^2_{3,1,1} &= \sigma_3^2+\frac{d_1^2\lg^2 d_1-d_0^2\lg^2 d_0}{0.01\beta_3^{-2}\left(d_1^2-d_0^2\right)}+\frac{25\beta_3^2}{\ln^2 10}\\ &\quad-100\beta_3^2M^2_{3,1,1}\\ P_1\left(3,1\right) &= \frac{d_1^2-d_0^2}{R_c^2-d_0^2}\\ M_{3,1,1} &= \frac{d_1^2\lg d_1-d_0^2\lg d_0}{d_1^2-d_0^2}.\end{cases} \tag{83}$$

$$\begin{cases}\mu_{3,1,2} &= \left(\ln 2-\ln a_2-0.25\right)\frac{10\beta_3}{\ln 10}\\ &\quad+\alpha_3-\frac{10\beta_3M_{3,1,2}}{\ln 10\sqrt{\pi}}\\ \sigma^2_{3,1,2} &= \frac{50\beta_3^2\sigma^2_{S_3}}{(\ln 10)^2}\\ &\quad+\frac{100\beta_3^2N_{3,1,2}}{\sqrt{\pi}\ln 10}+\frac{(\ln 2-\ln a_2-0.25)100\beta_3^2M_{3,1,2}}{\sqrt{\pi(\ln 10)^2}}\\ &\quad+\frac{100\beta_3^2M^2_{3,1,2}}{\pi}\\ P_2\left(3,1\right) &= \frac{1}{R_c^2-d_0^2}\begin{pmatrix}\frac{2d_1e^{-a_2d_1}}{a_2}+\frac{2d_0e^{-a_2d_0}}{a_2}\\ -\frac{2e^{-a_2d_1}}{a_2^2}+\frac{2e^{-a_2d_0}}{a_2^2}\end{pmatrix}\\ M_{3,1,2} &= \frac{Q_{X,3,1,2,1}-Q_{X,3,1,2,2}}{Q_{E,3,1,2}}\\ N_{3,1,2} &= \frac{\lg d_1Q_{X,3,1,2,1}-\lg d_0Q_{X,3,1,2,2}}{Q_{E,3,1,2}}\\ Q_{E,3,1,2} &= \mathrm{erf}\left(d_1-\ln 2+\ln a_2+0.25\right)\\ &\quad-\mathrm{erf}\left(d_0-\ln 2+\ln a_2+0.25\right)\\ Q_{X,3,1,2,1} &= e^{-0.5(d_1-\ln 2+\ln a_2+0.25)^2}\\ Q_{X,3,1,2,2} &= e^{-0.5(d_0-\ln 2+\ln a_2+0.25)^2}.\end{cases} \tag{84}$$

4) NLoS state $n=3,m=2$,

$$\begin{cases}\mu_{Y_{3,2}} &= P_1\left(3,2\right)\mu_{3,2,1}-P_2\left(3,2\right)\mu_{3,2,2}\\ \sigma^2_{Y_{3,2}} &= \mu^2_{Y_{3,2}}+P_1\left(3,2\right)\left(\sigma^2_{3,2,1}-\mu^2_{3,2,1}\right)\\ &\quad-P_2\left(3,2\right)\left(\sigma^2_{3,2,2}-\mu^2_{3,2,2}\right)\\ P\left(3,2\right) &= P_1\left(3,2\right)-P_2\left(3,2\right),\end{cases}$$

where

$$\begin{cases}\mu_{3,2,1} &= \frac{10(\ln 2-\ln a_1-0.25)\beta_3}{\ln 10}+\alpha_3-\frac{10\beta_3M_{3,1,2}}{\ln 10\sqrt{\pi}}\\ \sigma^2_{3,2,1} &= \frac{50\beta_3^2\sigma^2_{S_3}}{(\ln 10)^2}+\frac{100\beta_3^2N_{3,2,1}}{\sqrt{\pi}\ln 10}\\ &\quad+\frac{(\ln 2-\ln a_1-0.25)100\beta_3^2M_{3,2,1}}{\sqrt{\pi(\ln 10)^2}}+\frac{100\beta_3^2M^2_{3,2,1}}{\pi}\\ P_1\left(3,2\right) &= \frac{e^{b_1}}{R_c^2-d_0^2}\begin{pmatrix}-\frac{2d_1e^{-a_1R_c}}{a_1}+\frac{2d_1e^{-a_1d_1}}{a_1}\\ -\frac{2e^{-a_1R_c}}{a_1^2}+\frac{2e^{-a_1d_1}}{a_1^2}\end{pmatrix}\\ M_{3,2,1} &= \frac{Q_{X,3,2,1,1}-Q_{X,3,2,1,2}}{Q_{E,3,2,1}}\\ N_{3,2,1} &= \frac{\lg R_cQ_{X,3,2,1,1}-\lg d_1Q_{X,3,2,1,2}}{Q_{E,3,2,1}}\\ Q_{E,3,2,1} &= \mathrm{erf}\left(R_c-\ln 2+\ln a_1+0.25\right)\\ &\quad-\mathrm{erf}\left(d_1-\ln 2+\ln a_1+0.25\right)\\ Q_{X,3,2,1,1} &= e^{-0.5(R_c-\ln 2+\ln a_1+0.25)^2}\\ Q_{X,3,2,1,2} &= e^{-0.5(d_1-\ln 2+\ln a_1+0.25)^2},\end{cases} \tag{85}$$

$$\begin{cases}\mu_{3,2,2} &= \frac{10(\ln 2-\ln a_3-0.25)\beta_3}{\ln 10}+\alpha_3-\frac{10\beta_3M_{3,1,2}}{\ln 10\sqrt{\pi}}\\ \sigma^2_{3,2,2} &= \frac{50\beta_3^2\sigma^2_{S_3}}{(\ln 10)^2}+\frac{100\beta_3^2N_{3,2,1}}{\sqrt{\pi}\ln 10}\\ &\quad+\frac{(\ln 2-\ln a_1-0.25)100\beta_3^2M_{3,2,1}}{\sqrt{\pi(\ln 10)^2}}+\frac{100\beta_3^2M^2_{3,2,1}}{\pi}\\ P_2\left(3,2\right) &= \frac{e^{b_1}}{R_c^2-d_0^2}\begin{pmatrix}-\frac{2d_1e^{-a_3R_c}}{a_3}+\frac{2d_1e^{-a_3d_1}}{a_3}\\ -\frac{2e^{-a_3R_c}}{a_3^2}+\frac{2e^{-a_3d_1}}{a_3^2}\end{pmatrix},\end{cases} \tag{86}$$

This article has been accepted for publication in a future issue of this journal, but has not been fully edited. Content may change prior to final publication. Citation information: DOI 10.1109/TVT.2018.2881318, IEEE Transactions on Vehicular Technology

where

$$\begin{cases} a_3 & = a_1 + a_2 \\ M_{3,2,2} & = \frac{Q_{X,3,2,1,1} - Q_{X,3,2,1,2}}{Q_{E,3,2,1}} \\ N_{3,2,2} & = \frac{\lg R_c Q_{X,3,2,1,1} - \lg d_1 Q_{X,3,2,1,2}}{Q_{E,3,2,1}} \\ \mathrm{Q_{E,3,2,1}} & = \mathrm{erf}\left(R_c - \ln 2 + \ln a_3 + 0.25\right) \\ & \quad -\mathrm{erf}\left(d_1 - \ln 2 + \ln a_3 + 0.25\right) \\ Q_{X,3,2,2,1} & = e^{-0.5(R_c - \ln 2 + \ln a_3 + 0.25)^2} \\ Q_{X,3,2,2,2} & = e^{-0.5(d_1 - \ln 2 + \ln a_3 + 0.25)^2}. \end{cases} \quad (87)$$

APPENDIX E
PROOF OF (46)

According to the previous analysis, the distribution of the propagation loss given $N = 2, M = 1$ and its approximation can be expressed as

$$f_{Y|N,M}\left(y|2,1\right) = \int_{P_{L,d_0}}^{P_{L,d_1}} \left(\frac{2\beta_2^{-1} \ln 10 Q_E(y,z)}{10\left(R_c^2 - d_0^2\right)\sqrt{2\pi\sigma_{S_2}^2}} \right) dz \quad (88)$$

$$g_{Y|N,M}\left(y|2,1\right) = \frac{1}{\sqrt{2\pi\sigma_{Y_{2,1}}^2}} \exp\left(-\frac{\left(y - \mu_{Y_{2,1}}\right)^2}{2\sigma_{Y_{2,1}^2}} \right) \quad (89)$$

where $P_{L,d_0} = \alpha_2 + 10\beta_2 \lg d_0$,$P_{L,d_1} = \alpha_2 + 10\beta_2 \lg d_1$ and $Q_E\left(y,z\right) = \exp\left(-\frac{(y-z)^2}{2\sigma_{S_2}^2} - \alpha_2 e^{\frac{z \ln 10}{10\beta_2}} + \frac{z \ln 10}{5\beta_2} \right)$. Then the KL-divergence from $f_{Y|N,M}\left(y|2,1\right)$ to $g_{Y|N,M}\left(y|2,1\right)$ can be expressed as

$$\begin{aligned} & KL\left(g_{Y|N,M}\left(y|2,1\right) || f_{Y|N,M}\left(y|2,1\right)\right) \\ & = \int_{-\infty}^{+\infty} g_{Y_{2,1}}\left(y\right) \ln g_{Y_{2,1}}\left(y\right) dy \\ & - \int_{-\infty}^{+\infty} g_{Y|N,M}\left(y|2,1\right) \ln f_{Y|N,M}\left(y|2,1\right) dy \\ & = KL_I + KL_{II}, \end{aligned} \quad (90)$$

where

$$KL_I = \ln \frac{1}{\sqrt{2\pi\sigma_{Y_{2,1}}^2}} - 0.5, \quad (91)$$

$$\begin{aligned} KL_{II} &= -\ln \frac{2\beta_2^{-1} \ln 10}{10\left(R_c^2 - d_0^2\right)\sqrt{2\pi\sigma_{S_2}^2}} \\ &= -\ln \frac{2\beta_2^{-1} \ln 10}{10\left(R_c^2 - d_0^2\right)\sqrt{2\pi\sigma_{S_2}^2}} + KL_{II_2}, \end{aligned} \quad (92)$$

where

$$KL_{II_2} = -\int_{-\infty}^{+\infty} \left[\begin{array}{c} \frac{1}{\sqrt{2\pi\sigma_{Y_{2,1}}^2}} \exp\left(-\frac{\left(y - \mu_{Y_{2,1}}\right)^2}{2\sigma_{Y_{2,1}^2}} \right) \\ \ln\left[\int_{P_{L,d_0}}^{P_{L,d_1}} Q_E\left(y,z\right) dz \right] \end{array} \right] dy.$$

According to Jensen's inequality

$$\begin{aligned} KL_{II_2} &\le -\int_{-\infty}^{+\infty} \left[\begin{array}{c} \frac{10\beta_2(\lg d_1 - \lg d_0)}{\sqrt{2\pi\sigma_{Y_{21}}^2}} \exp\left(-\frac{\left(y - \mu_{Y_{21}}\right)^2}{2\sigma_{Y_{21}^2}} \right) \\ \left[\int_{P_{L,d_0}}^{P_{L,d_1}} \ln\left(\frac{0.1\beta_2^{-1}}{\lg d_1 - \lg d_0} Q_E\left(y,z\right) \right) dz \right] \end{array} \right] dy \\ &= \frac{\sigma_{L_{2,1}}^2 + \left(\alpha_2 - \mu_{L_{2,1}}\right)^2}{2\sigma_{S_2}^2} + \frac{5\beta_2\left(\alpha_2 - \mu_{L_{21}}\right)}{\sigma_{S_2}^2 \ln 10}\left(\ln d_1 + \ln d_0\right) \\ &+ \frac{50\beta_2^2}{3\sigma_{S_2}^2 \ln^2 10}\left(\ln^2 d_1 + \ln d_1 \ln d_0 + \ln^2 d_0\right). \end{aligned} \quad (93)$$

Then the upper bound of the KL-divergence can be obtained as shown in (46).

REFERENCES

[1] J. G. Andrews, S. Buzzi, W. Choi, S. V. Hanly, A. Lozano, A. C. K. Soong, and J. C. Zhang, "What will 5G be?" *IEEE Journal on Selected Areas in Communications*, vol. 32, no. 6, pp. 1065–1082, Jun. 2014.

[2] S. Rangan, T. S. Rappaport, and E. Erkip, "Millimeter-wave cellular wireless networks: Potentials and challenges," *Proceedings of the IEEE*, vol. 102, no. 3, pp. 366–385, Mar. 2014.

[3] Z. Pi and F. Khan, "An introduction to millimeter-wave mobile broadband systems," *IEEE Communications Magazine*, vol. 49, no. 6, pp. 101–107, Jun. 2011.

[4] T. S. Rappaport, S. Sun, R. Mayzus, H. Zhao, Y. Azar, K. Wang, G. N. Wong, J. K. Schulz, M. Samimi, and F. Gutierrez, "Millimeter wave mobile communications for 5G cellular: It will work!" *IEEE Access*, vol. 1, pp. 335–349, 2013.

[5] M. R. Akdeniz, Y. Liu, M. K. Samimi, S. Sun, S. Rangan, T. S. Rappaport, and E. Erkip, "Millimeter wave channel modeling and cellular capacity evaluation," *IEEE Journal on Selected Areas in Communications*, vol. 32, no. 6, pp. 1164–1179, Jun. 2014.

[6] Y. Azar, G. N. Wong, K. Wang, R. Mayzus, J. K. Schulz, H. Zhao, F. Gutierrez, D. Hwang, and T. S. Rappaport, "28 GHz propagation measurements for outdoor cellular communications using steerable beam antennas in new york city," in *2013 IEEE International Conference on Communications (ICC)*, Jun. 2013, pp. 5143–5147.

[7] S. Nie, G. R. MacCartney, S. Sun, and T. S. Rappaport, "28 ghz and 73 ghz signal outage study for millimeter wave cellular and backhaul communications," in *Communications (ICC), 2014 IEEE International Conference on*. IEEE, 2014, pp. 4856–4861.

[8] J. Meinilä, P. Kyösti, T. Jämsä, and L. Hentilä, *WINNER II channel models*. Hoboken, NJ, USA: Wiley-Blackwell, 2009, pp. 39–92.

[9] T. Bai, R. Vaze, and R. W. Heath, "Analysis of blockage effects on urban cellular networks," *IEEE Transactions on Wireless Communications*, vol. 13, no. 9, pp. 5070–5083, Sep. 2014.

[10] J. G. Andrews, T. Bai, M. N. Kulkarni, A. Alkhateeb, A. K. Gupta, and R. W. Heath, "Modeling and analyzing millimeter wave cellular systems," *IEEE Transactions on Communications*, vol. 65, no. 1, pp. 403–430, Jan. 2017.

[11] K. B. Baltzis, "Analytical and closed-form expressions for the distribution of path loss in hexagonal cellular networks," *Wireless Personal Communications*, vol. 60, no. 4, pp. 599–610, 2011.

[12] Z. Bharucha and H. Haas, "The distribution of path losses for uniformly distributed nodes in a circle," *Rec. Lett. Commun.*, vol. 2008, pp. 4:1–4:4, Jan. 2008.

[13] S. Baroudi and Y. R. Shayan, "Outage probability in a circle with uniformly distributed users," in *2012 25th IEEE Canadian Conference on Electrical and Computer Engineering (CCECE)*, Apr. 2012, pp. 1–4.

[14] M. Abdulla and Y. R. Shayan, "Large-scale fading behavior for a cellular network with uniform spatial distribution," *Wireless Communications and Mobile Computing*, vol. 16, no. 7, pp. 748–764, Dec. 2016.

[15] X. Yan, J. Xu, Y. Zhu, J. Wang, Y. Yang, and C. X. Wang, "Downlink average rate and sinr distribution in cellular networks," *IEEE Transactions on Communications*, vol. 64, no. 2, pp. 847–862, Feb. 2016.

[16] M. Abdulla and Y. R. Shayan, "Closed-form path-loss predictor for gaussianly distributed nodes," in *2010 IEEE International Conference on Communications (ICC)*, May 2010, pp. 1–6.

[17] ——, "An exact path-loss density model for mobiles in a cellular system," in *ACM International Symposium on Mobility Management and Wireless Access*, 2009, pp. 118–122.

[18] K. B. Baltzis, "Closed-form description of microwave signal attenuation in cellular systems," *Radioengineering*, vol. 19, no. 1, pp. 11–16, Apr. 2010.
[19] J. Xu, X. Yan, Y. Zhu, J. Wang, Y. Yang, X. Ge, G. Mao, and O. Tirkkonen, "Statistical analysis of path losses for sectorized wireless networks," *IEEE Transactions on Communications*, vol. 65, no. 4, pp. 1828–1838, Apr. 2017.
[20] T. Bai and R. W. Heath, "Coverage and rate analysis for millimeter-wave cellular networks," *IEEE Transactions on Wireless Communications*, vol. 14, no. 2, pp. 1100–1114, Feb. 2015.
[21] M. D. Renzo, "Stochastic geometry modeling and analysis of multi-tier millimeter wave cellular networks," *IEEE Transactions on Wireless Communications*, vol. 14, no. 9, pp. 5038–5057, Sep. 2015.
[22] X. Ge, B. Yang, J. Ye, G. Mao, C. X. Wang, and T. Han, "Spatial spectrum and energy efficiency of random cellular networks," *IEEE Transactions on Communications*, vol. 63, no. 3, pp. 1019–1030, Mar. 2015.
[23] M. Ding, P. Wang, D. Lpez-Prez, G. Mao, and Z. Lin, "Performance impact of LoS and NLoS transmissions in dense cellular networks," *IEEE Transactions on Wireless Communications*, vol. 15, no. 3, pp. 2365–2380, Mar. 2016.
[24] T. Ding, M. Ding, G. Mao, Z. Lin, D. Lpez-Prez, and A. Y. Zomaya, "Uplink performance analysis of dense cellular networks with LoS and NLoS transmissions," *IEEE Transactions on Wireless Communications*, vol. 16, no. 4, pp. 2601–2613, Apr. 2017.
[25] J. G. Andrews, F. Baccelli, and R. K. Ganti, "A tractable approach to coverage and rate in cellular networks," *IEEE Transactions on Communications*, vol. 59, no. 11, pp. 3122–3134, Nov. 2011.
[26] T. S. Rappaport, Y. Xing, G. R. MacCartney, A. F. Molisch, E. Mellios, and J. Zhang, "Overview of Millimeter Wave Communications for Fifth-Generation (5G) Wireless Networks–With a Focus on Propagation Models," *IEEE Transactions on Antennas and Propagation*, vol. 65, no. 12, pp. 6213–6230, Dec. 2017.
[27] A. Goldsmith, *Wireless Communications*. New York, NY, USA: Cambridge University Press, 2005.
[28] M. K. Samimi, T. S. Rappaport, and G. R. MacCartney, "Probabilistic omnidirectional path loss models for millimeter-wave outdoor communications," *IEEE Wireless Communications Letters*, vol. 4, no. 4, pp. 357–360, Aug. 2015.
[29] J. Li, "Los probability modeling for 5G indoor scenario," in *2016 International Symposium on Antennas and Propagation (ISAP)*, Oct. 2016, pp. 204–205.
[30] S. Kullback and R. A. Leibler, "On information and sufficiency," *Annals of Mathematical Statistics*, vol. 22, no. 22, pp. 79–86, Mar. 1951.
[31] G. L. Stüber, *Principles of mobile communication*. Springer Science & Business Media, 2011.
[32] Y. Singer and M. K. Warmuth, "Batch and on-line parameter estimation of gaussian mixtures based on the joint entropy," in *Proceedings of the 1998 Conference on Advances in Neural Information Processing Systems II*. Cambridge, MA, USA: MIT Press, 1999, pp. 578–584.
[33] T. Steihaug, "The conjugate gradient method and trust regions in large scale optimization," *Siam Journal on Numerical Analysis*, vol. 20, no. 3, pp. 626–637, Jun. 1983.
[34] S. Sun, H. Yan, G. R. MacCartney Jr, and T. S. Rappaport, "Millimeter wave small-scale spatial statistics in an urban microcell scenario," in *IEEE International Conference on Communications (ICC)*, May. 2017, pp. 1–7.